



# Bioactive glass beads as a route to passive drug delivery

Marie Sykes<sup>1</sup> · Casey Schwarz<sup>1</sup> · Rashi Sharma<sup>2</sup> · Eric Bissell<sup>3</sup> · Kathleen Richardson<sup>2</sup> · Parag Banerjee<sup>3</sup>

Received: 13 February 2024 / Accepted: 15 May 2024

© The Author(s), under exclusive licence to The Materials Research Society 2024

## Abstract

Bioactive glass microbeads are emerging as an attractive method for sustained drug release over extended periods, ranging from several hours to weeks, and across diverse applications such as toothpaste and bone repair. Their effectiveness stems from their capacity to be engineered into uniquely adaptable structures such as fibers, beads, and mesh scaffolding. In this investigation, bioactive glass microbeads ( $\text{SiO}_2\text{-B}_2\text{O}_3$ ) with a distinctive hollow core and porous shell structure were employed. The morphology of the beads was characterized in detail using optical microscopy, scanning electron microscopy, x-ray diffraction, Raman spectroscopy, and surface interferometry. The drug loading and passive diffusion of the beads was monitored through UV–Vis spectroscopy. This study reveals favorable morphology, robust structure, and efficient passive diffusion of these microbeads. These attributes indicated a new route to transdermal medication release.

## Introduction

Sustained or controlled drug release is a method used in the pharmaceutical and medical fields to ensure that a therapeutic dose of a drug is consistently delivered over an extended period of time, maintaining a steady and effective concentration in the body [1]. During this process, there is an “*initial burst*”, where the drug is released quickly. This burst is then followed by a “*maintained release*” at a certain concentration. This provides an immediate therapeutic effect followed by a maintained and controlled drug administration. This may reduce frequency of administrations, mitigate side effects, and allows for controlled site administration. There are various drug delivery system, some used internally and externally. These may include implants, microspheres, liposomes, and patches [2, 3]. The choice of system depends on factors like the drug’s properties, desired release profile, and the specific medical condition being treated [2, 4].

Bioactive glasses were discovered in 1969 by Hench [5] and have since been used in regenerative medicine, dentistry, treatment of infections, and drug delivery [4, 6, 7]. These glasses are based on the composition  $\text{Na}_2\text{O}$ ,  $\text{CaO}$ ,  $\text{P}_2\text{O}_5$ , and  $\text{SiO}_2$  system and possess desirable properties such as bioactivity, biocompatibility, bioinert behavior, and antibacterial properties [8]. These materials can also be engineered to be used in many forms, sizes and shapes (such as bulk, powder, fibers or beads) depending on desired application [9].

In our research, we investigated bioactive glass microbeads (BGBs) with a hollow core and porous shell. Since the bead’s surface area, porosity, core size and durability will determine its potential for use as drug delivery system [9, 10]. The microbeads were characterized using optical microscopy, scanning electron microscopy (SEM), Raman spectroscopy, x-ray diffraction (XRD), and interferometry before demonstrating a method for successful drug loading and sustained delivery in solution.

## Materials and methods

### Bioactive beads

The bioactive beads (OL-GL (1756b)) used in this study were purchased from Mo-Sci Corp (Rolla, MO). The beads were stated to range in diameter from 38 to 90  $\mu\text{m}$ . A silica base ( $\text{SiO}_2$ ) composed 75–90% of the bead composition

✉ Casey Schwarz  
cschwarz@ursinus.edu

<sup>1</sup> Physics and Astronomy, Ursinus College, 601 E Main St, Collegeville, PA 19426, USA

<sup>2</sup> Center of Optics and Photonics, CREOL University of Central Florida, 4304 Scorpius Street, Orlando, FL 32816, USA

<sup>3</sup> Materials Science & Engineering, University of Central Florida, Orlando, FL 32816, USA

and a secondary component boron oxide ( $B_2O_3$ ) composed 5.0–15%, the other 1.0–10% is listed as unknown composition. The bulk density of the dry beads are roughly 0.35–0.40 g/cm<sup>3</sup>, the pore size ranges from 10 to 300 nm with a porosity equal to or over 90%, and the shell thickness is around 1  $\mu$ m [11, 12].

### Characterization and metrology

A Nikon C2 confocal microscope was used to capture images of the dry beads, beads in solution and filled beads in solution and monitor changes in size, morphology, and diffusion. Absorption was measured using a Jasco V-670 UV–VIS–NIR Molecular Absorption Spectrometer. A NewView™ 9000 3D optical surface profiler was used to provide non-contact optical surface profiling of the shells of the dry beads. The measurements were nondestructive and needed no sample preparation. A Scanning Electron Microscope (SEM), Zeiss N-Vision 40 was used to image uncoated dry beads at an accelerating voltage of 5 kV. This was done to confirm the bead dimensions, surface morphology, additionally; beads were broken in half for shell measurements. Raman microscopy was performed to examine the chemical structure and crystallinity of the beads. The Raman system used was a Horiba LabRAM HR Evolution Nano. Measurements were conducted using a wavelength of 785 nm, laser power of 30 W, a 20  $\mu$ m spot size (10 $\times$  magnification objective) and a 20 s acquisition time. X-ray diffraction (XRD) was performed using a PANalytical Empyrean system on whole and powdered bead samples.

### Methods and analysis

In order to measure passive diffusion of a core-filled liquid from the center of the beads, beads were dyed, filtered, dried, immersed in solution and their release was monitored via UV–Vis spectroscopy. The beads were dyed by placing them into high saturations of blue cell stain (combination of methanol solution and phosphate buffered saline (PBS)

(5  $\mu$ L of cell dye in 300  $\mu$ L of PBS) for three days. The dye molecules used in the work was comparable in size (1–2 nm) of therapeutic drugs used in encapsulated beads in other works [13–15]. The beads were then filtered for two hours after the PBS-stain solution was poured over a filter paper (Ahlstrom 615 fast filter grade with 235 mL/min rapidity) and rinsed with 100–200  $\mu$ L of fresh PBS. The BGBs then dried for one day at room temperature to minimize any breakage and loss of sample due to cohesion to the wet filter. To take data to measure the rate of passive diffusion from the BGBs into their environment, 1–4.5 mg of dyed and drained beads were placed into a cuvette with 150  $\mu$ L of fresh PBS inside a 6Q quartz cuvette. Over the course of a day, absorption measurements were observed over a range of 350–800 nm with the most intense peak developing at 654 nm. The samples were placed in a cuvette where the spectrometer would measure the absorption value at 654 nm once every five minutes over the course of 54.5 h. No animals or humans were tested on during this research.

### Results and discussion

Figure 1 displays optical images of the dry bioactive beads (Fig. 1a) and core-filled beads in PBS (Fig. 1b). These images confirmed the specified size distribution, with most beads remaining intact after handling. The optical images of the dried beads were used in combination with SEM imaging to confirm size, distribution and morphology. The measured sizes of the beads range from approximately 33 to 111 nm with 86% beads falling between the ranges of 60 and 105 nm, this is slightly outside of the reported 38–90  $\mu$ m (Fig. 1c) [11, 12]. Blue dye core-filled beads are seen within solution and can be compared to unfilled beads (Fig. 1b). Bead cores were considered filled though optical observation, however, further investigation would need to be conducted in order to obtain exact fill percentages. Compared to initial studies on similar compositions of solid beads and solid porous fragments of bioactive glass, the filling of the hollow beads in this paper was obvious.

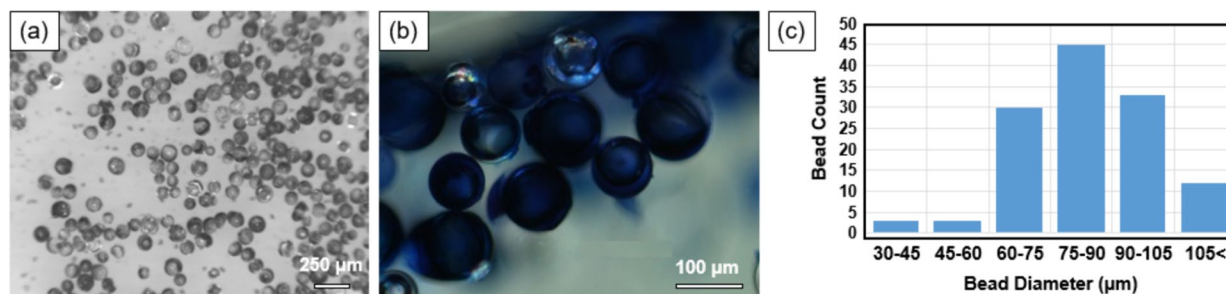


**Fig. 1** Optical images of the **a** dry bioactive beads and **b** core-filled beads in PBS. **c** Histogram showing most bead diameters were found to be in the ranges of 60 to 105  $\mu$ m

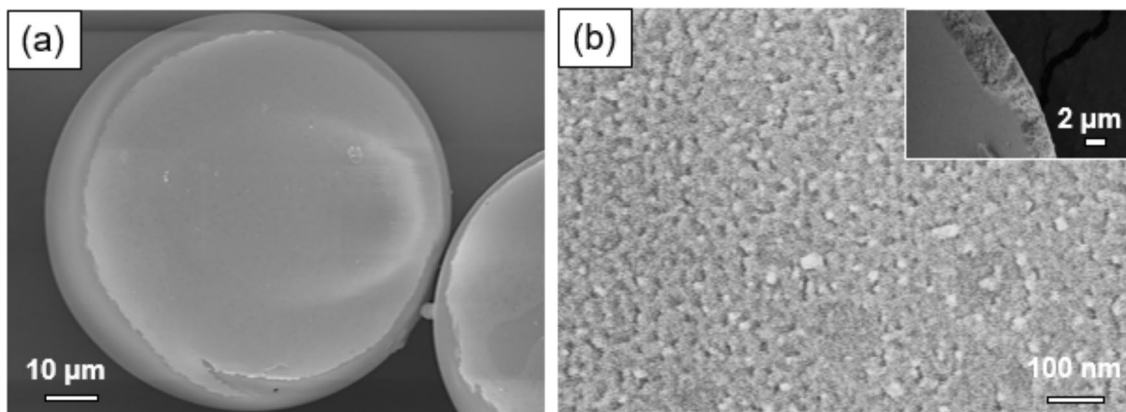


**Fig. 2** SEM images of **a** a whole, intact dry bioactive bead measuring 72 µm, **b** a detailed look at the bead’s shell showing pores with inset image of a cracked shell, showing a thickness ranging from 1 to 3 µm and detailed porosity

**Fig. 3** **a** XRD measurement and **b** Raman measurement of powdered beads

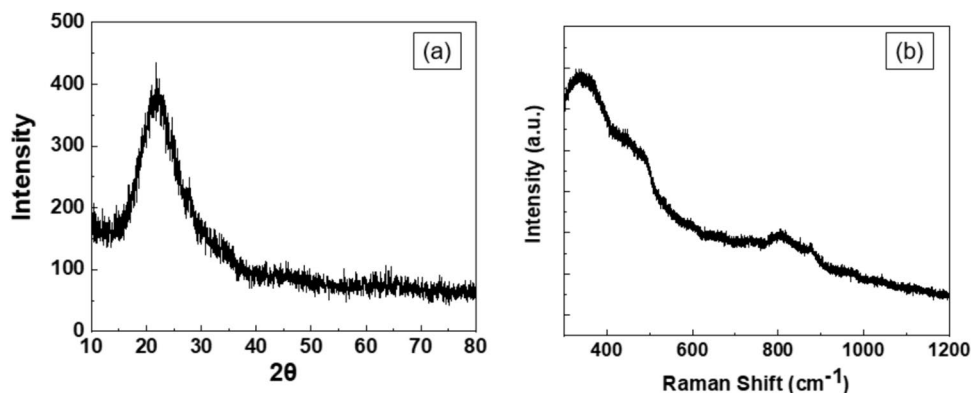
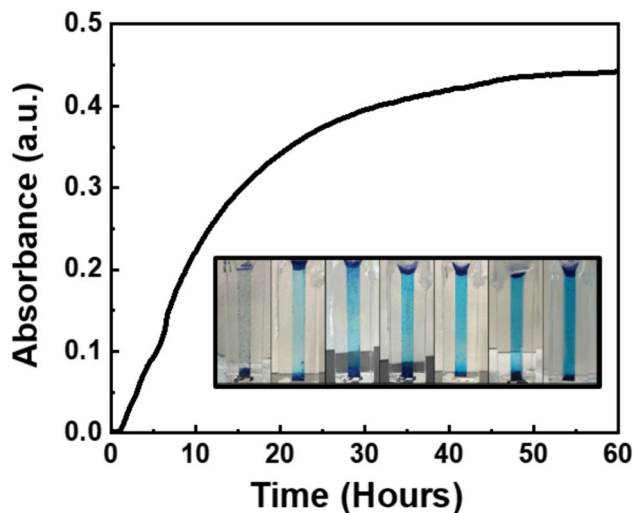


Figure 2 shows SEM analysis of the dry bioactive glass beads at different magnifications with an inset profile image of a cracked shell in order to investigate thickness and porosity of the shell. Optical surface profiler imagery of the dry bioactive beads was used to measure diameter, roughness and homogeneity across the shells. The root mean squared (rms) surface roughness of the surface of the bead shell was measured to be  $12.435 \pm 2.41 \mu\text{m}$ . Roughness was therefore considered homogeneous across the shell of the bead and small, indicating small pore sizes. The dimensional profiles were also consistent with measured diameters of the beads using optical microscopy and SEM. XRD characterization (Fig. 3a) confirmed the vitreous nature of the powdered beads showing the pattern shape typical amorphous phase pattern shape below  $400 \text{ cm}^{-1}$  with no crystallization peaks [16]. Raman spectra (Fig. 3b) show broad peaks typical of bioactive glass compositions found in the literature [17].

A sustained drug delivery profile was obtained by using micron sized bioactive glass beads as delivery vehicle for blue cell dye over a 60 h timeframe (Fig. 4). The initial burst drug release is seen from 0 to 20 h where absorbency has a measured change in absorption values of 0–0.34 accounting



**Fig. 4** Measured UV–Vis absorption (arbitrary units) vs time in hours of core-filled beads in PBS solution. Inset is an image of core-filled beads dispersed in fresh PBS solution inside the cuvette as a function of time

for its greatest change in drug release of  $\Delta 77\%$ . From 20 to 40 h, a gradual slowdown of release was observed as measured absorbance values change from 0.34 to 0.42 ( $\Delta 18\%$ ). During the final stage, from 40 to 60 h, absorbency only changed from 0.42 to 0.44 ( $\Delta 5\%$ ), indicating maximum drug release levels have been achieved.

The bioactive microbead samples used throughout this study were found to be robust, being able to be handled, washed, and filtered without losing shape, size and structure. The surface of the beads was found to be homogeneously porous with low roughness. The highly porous shell and surface area of the microbeads could aid in diffusion of a drug solution [14, 18]. Additionally, the pores could also act as reservoirs for drug molecules, depending on application. More characterization is needed, including thermal, chemical, and crystallinity of the microbeads [11, 12]. Future work would include analysis of post-release beads, testing shell thickness and porosity as a function of release and percentage fill, additional drug solutions, applying mathematical concentration models to spectra, and testing over longer periods of time [18, 19].

**Acknowledgments** This work was supported by the UC Department of Physics and Astronomy and the University of Central Florida's College of Optics and Photonics Optical Materials Laboratory under Professor Kathleen Richardson.

**Authors contributions** Not applicable.

**Funding** This work was supported by the Ursinus College (UC) Student Research Fund, the UC Summer Fellows 2022, and the 2022 ACerS student travel grant.

**Data availability** Data can be made available upon request to Casey Schwarz, cschwarz@ursinus.edu.

## Declarations

**Conflict of interest** The authors declare no conflict of interest.

## References

1. A.M. El-Kady, M.M. Farag, Bioactive glass nanoparticles as a new delivery system for sustained 5-fluorouracil release: Characterization and evaluation of drug release mechanism. *J. Nanomater.* **16**, 839207 (2015)
2. F. Baine, S. Hamzehlou, S. Kargozar, Bioactive glasses: where are we and where are we going? *J. Funct. Biomater.* **9**(1), 25 (2018)
3. N. Dey, F.P. Mohony, G.B. Reshma, D. Rao, M. Ganguli, D. Santhiya, Bioinspired synthesis of bioactive glass nanocomposites for hyaluronic acid delivery to bone and skin. *Int. J. Biol. Macromol.* **253**, 6 (2023)
4. M. Cannio, D. Bellucci, J.A. Roether, D.N. Boccaccini, V. Cannillo, Review bioactive glass applications: a literature review of human clinical trials. *Materials* **14**, 5440 (2021)
5. L.L. Hench, R.J. Splinter, W.C. Allen, T.K. Greenlee, Bonding mechanisms at the Interface of ceramic prosthetic materials. *J. Biomed. Mater. Res.* **5**(6), 117 (1971)
6. E. Sharifi, A. Bigham, S. Yousefiasl, M. Trovato, M. Ghomi, Y. Esmaeili, P. Samadi, A. Zarrabi, M. Ashrafizadeh, S. Sharifi, Mesoporous bioactive glasses in cancer diagnosis and therapy: stimuli-responsive, toxicity, immunogenicity, and clinical translation. *Adv. Sci.* **9**(2), 2102678 (2022)
7. C. Soundrapandian, S. Datta, B. Kundu, D. Basu, B. Sa, Porous bioactive glass scaffolds for local drug delivery in osteomyelitis: development and in vitro characterization. *AAPS Pharm. Sci. Tech.* **11**, 4 (2010)
8. P.A. Dash, S. Mohanty, S.K. Nayak, A review on bioactive glass, its modifications and applications in healthcare sectors. *J. Non-Cryst. Solids* **614**, 122404 (2023)
9. S. Gupta, S. Majumdar, S. Krishnamurthy, Bioactive glass: a multifunctional delivery system. *J. Control. Release* **335**, 481 (2021)
10. M. Sykes, R. Sharma, Applying bioactive glass beads for long-term drug delivery. *Phys. Astron. Present.* **18**, 1 (2023)
11. K. Li, G.M. Veith, M.E. Lamm et al., Hermetically sealed porous-wall hollow microspheres enabled by monolithic glass coatings: potential for thermal insulation applications. *Vacuum* **195**, 110667 (2022)
12. M.E. Lamm, K. Li, J. Atchley et al., Tailorable thermoplastic insulation foam composites enabled by porous-shell hollow glass spheres and expandable thermoplastic microspheres. *Polymer* **267**, 125652 (2023)
13. X. Wang, W. Li, Biodegradable mesoporous bioactive glass nanospheres for drug delivery and bone tissue regeneration. *Nanotechnology* **27**, 225102 (2016)
14. J. Hum, A.R. Boccaccini, Bioactive glasses as carriers for bioactive molecules and therapeutic drugs: a review. *J. Mater. Sci.: Mater. Med.* **23**, 2317–2333 (2012)
15. L. Francis, D. Meng, J.K. Knowles et al., Multi-functional P(3HB) microsphere/45S5 bioglass®-based composite scaffolds for bone tissue engineering. *Acta Biomater.* **6**(7), 2773–2786 (2010)
16. K. Schickle, K. Zurlinden, C. Bergmann et al., Synthesis of novel tricalcium phosphate-bioactive glass composite and functionalization with rhBMP-2. *J. Mater. Sci.: Mater. Med.* **22**, 763 (2011)
17. A. Balamurugan, G.D. Sockalingum, J. Michel et al., Synthesis characterisation of sol gel derived bioactive glass for biomedical applications. *Mater. Lett.* **60**, 3752 (2006)
18. C. Wu, J. Change, Mesoporous bioactive glasses: structure characteristics, drug/growth factor delivery and bone regeneration application. *Interface Focus* **2**, 292–306 (2012)
19. L. Ruan, M. Su, X. Qin et al., Progress in the application of sustained-release drug microspheres in tissue engineering. *Mater. Today Bio* **16**, 100394 (2022)

**Publisher's Note** Springer Nature remains neutral with regard to jurisdictional claims in published maps and institutional affiliations.

Springer Nature or its licensor (e.g. a society or other partner) holds exclusive rights to this article under a publishing agreement with the author(s) or other rightsholder(s); author self-archiving of the accepted manuscript version of this article is solely governed by the terms of such publishing agreement and applicable law.